Reac Kinet Mech Cat (2018) 124:545–561
https://doi.org/10.1007/s11144-018-1372-6

Fischer–Tropsch synthesis over various Fe/Al_2O_3–Cr_2O_3 catalysts

Pawel Mierczynski[1] · Bartosz Dawid[1] · Waldemar Maniukiewicz[1] · Magdalena Mosinska[1] · Mateusz Zakrzewski[1] · Radoslaw Ciesielski[1] · Adam Kedziora[1] · Sergey Dubkov[2] · Dmitry Gromov[2] · Jacek Rogowski[1] · Izabela Witonska[1] · Malgorzata I. Szynkowska[1] · Tomasz Maniecki[1]

Received: 20 November 2017 / Accepted: 10 February 2018 / Published online: 20 February 2018

Abstract Monometallic iron supported catalysts were prepared by the impregnation method and tested in Fischer–Tropsch (F–T) synthesis. The activity tests performed in the studied reaction showed that the composition of the catalyst strongly influences the reactivity of the catalytic systems in the F–T reaction. It was also found that the system which showed the highest content of iron species on the catalyst surface exhibited the highest yield in F–T reaction. In addition, the most active catalyst also showed high specific surface area, high total acidity value and the highest amount of iron species on the catalyst surface. The analysis of the liquid product of F–T synthesis confirmed the occurrence of aliphatic, branched and unsaturated linear hydrocarbons.

Keywords Fischer–Tropsch · Iron catalyst · CO hydrogenation · Binary oxide · Monometallic catalysts

Introduction

Currently, Fischer–Tropsch synthesis is considered to be the main alternative to fossil fuels. Undoubtedly, the advantage of this process is a possibility to the pure types of fuel production without any sulfur and nitrogen compounds [1, 2]. F–T synthesis is a well known process starting from 1920s and today increasing interest of usage is observed to obtain alternative feedstock of hydrocarbons such us fuels and waxes [3–6]. The composition of the final product obtained in F–T synthesis

✉ Pawel Mierczynski
pawel.mierczynski@p.lodz.pl; mierczyn25@wp.pl

[1] Lodz University of Technology, Lodz, Poland

[2] National Research University of Electronic Technology, Zelenograd, Russia

depends on the process conditions and the type of the catalyst used in the studied process. Besides the aliphatic, branched and unsaturated linear hydrocarbons, oxygen containing hydrocarbons like alcohols, aldehydes, ketones and acids can also be formed during this process. In addition, except the remaining hydrocarbons, which can be formed during the synthesis also the paraffin waxes can be produced via hydrogenation of CO [7].

The most commonly used catalysts in F–T synthesis are cobalt [8–10], nickel and iron [3, 5, 11–13].The typical composition of the syngas used during the FT synthesis realized on the catalytic system correspond to the molar ratio between H_2 and CO equal to 2. The wide distribution of organic compounds formed during the F–T process leads to the conclusion that it is needed to select appropriate catalytic systems in order to increase the selectivity to the desired products, such as petrol or diesel fractions. Generally, it is well known that iron catalysts are active systems in the F–T process [14]. Many researchers try to improve the catalytic properties by the addition of various promotors. Noble metal addition is one of the possibilities to improve selectivity, activity and stability of Fe system in F–T reaction. The typical supports used for the preparation of the catalytic systems are Al_2O_3, SiO_2, CeO_2, TiO_2, ZrO_2 and binary oxides, mixtures of previously mentioned oxides systems and zeolites. It should also be noted that catalysts supported on binary oxide systems showed higher specific surface area, mechanical strength and exhibited higher catalytic activity in various processes [15–19]. The selection of the specific composition of the binary system generates the change of their physicochemical properties in a certain direction.

In summary, all of these facts suggest that it is important to produce hydrocarbons via Fischer–Tropsch synthesis on Fe catalyst supported on binary oxide systems. In order to achieve the intended goal, we decided to synthesize monometallic iron supported catalysts by impregnation method and we studied their surface composition and the reactivity properties in the F–T process. Furthermore, the physicochemical properties of the prepared catalytic systems were also studied in this work using BET, TPR–H_2, SEM–EDS, TPD–NH_3 and TOF–SIMS methods.

Experimental part

Catalysts preparation

Monometallic iron supported catalysts supported on various Al_2O_3–Cr_2O_3 binary oxides system (Al:Cr = 2, 1, 0.5) were prepared by impregnation method using $Fe(NO_3)_3{\cdot}9H_2O$ as an active phase precursor. The supports which were used during the preparation step of the catalytic systems were prepared by co-precipitation method from appropriate aqueous solution of $Al(NO_3)_3{\cdot}9H_2O$ and $Cr(NO_3)_3{\cdot}9H_2O$. Ammonia was used as a precipitating agent during the co-precipitation process. The obtained supports were calcined for 4 h in air atmosphere at 400 °C. Whereas, the monometallic supported iron catalysts were calcined for 4 h in air atmosphere at 500 °C.

Specific surface area measurements

The BET surface area and porosity of the prepared supports and monometallic supported iron catalysts were determined in a sorptometer Sorptomatic 1900 apparatus.

FTIR measurements

The analysis of the liquid products formed during the F–T process were performed on an IRTracer-100 FTIR (Shimadzu) spectrometer equipped with liquid nitrogen cooled MCT detector. During all experiments, a resolution of 4.0 cm^{-1} was used and 128 scans were taken to achieve a satisfactory signal to noise ratio. For all measurements, the "Specac" ATR accessory was used.

SEM–EDS measurements

The morphology of the monometallic iron catalyst supported on Al_2O_3–Cr_2O_3 binary oxide system (Al:Cr = 2, 1, 0.5) were studied by S-4700 scanning electron microscope HITACHI (Japan), equipped with an energy dispersive spectrometer EDS (ThermoNoran, USA).

TPR–H_2 measurements

TPR–H_2 measurements were performed for both binary supports and the prepared monometallic iron supported catalysts using an automatic AMI-1 instrument in the temperature range 25–900 °C. The heating rates applying during the reduction process were 10 and 1 °C min^{-1} for supports and monometallic catalysts, respectively. The mass of the investigated catalyst was about 0.1 g in each test. During the reduction process the mixture of 5%H_2–95%Ar was used with a thermal conductivity detector.

Acidity measurements

The total acidity and the distributions of the acids centers for all the prepared catalysts which were previously reduced at 500 °C in a mixture of 5%H_2–95%Ar were studied by TPD–NH_3 technique. Before all experiments, each sample (about 0.2 g in each test) was reduced in situ in a mixture of 5%H_2–95%Ar at 500 °C for 1 h and then purified in situ in flowing He at 600 °C for 30 min^{-1}. Then the sample was cooled down to ambient temperature in a helium stream. In the next step, the physically adsorbed NH_3 was removed from the surface of the investigated catalyst in a helium stream at 100 °C. Then the chemisorbed NH_3 was monitored using thermal-conductivity detector (TCD) during the heating of the sample from 100 to 600 °C.

Phase composition studies

Phase composition studies for the monometallic iron supported catalysts after reduction were carried out using a PANalytical X'Pert Pro MPD diffractometer in Bragg–Brentano reflecting geometry. Cu K_α radiation from a sealed tube was applied during all measurements. During each experiment, a PANalytical X'Celerator detector was applied in the 2 Theta angle 5–90°. The ex situ XRD measurements were performed for reduced catalysts in a mixture of 5%H_2–95%Ar for 1 h at 500 °C.

ToF–SIMS measurements

The secondary ion mass spectra for the supports and monometallic iron catalyst were recorded using a TOF–SIMS IV mass spectrometer manufactured by Ion-Tof GmbH, Muenster, Germany. The instrument is equipped with a Bi liquid metal ion gun and a high mass resolution time of flight mass analyzer. Secondary ion mass spectra were recorded from an approximately 100 μm × 100 μm area of the spot surface. During measurements, the analyzed area was irradiated with the pulses of 25 keV Bi_3^+ ions at 10 kHz repetition rate and an average ion current 0.4 pA. The analysis time was 30 s giving an ion dose below static limit of 1×10^{13} ions cm^{-2}.

Catalytic activity tests

The F–T synthesis was carried out in a high-pressure fixed bed reactor using a gas mixture of H_2 and CO with molar ratio 2:1. The total flow of the reagents during the reaction was 90 mL min^{-1}. In each test, about 2 g of the catalyst was loaded into the fixed bed high pressure reactor. The F–T process was carried out under elevated pressure 30 atm in the temperature range 240–280 °C. Before each catalytic test, the catalysts were previously reduced in a mixture of 5%H_2–95%Ar for 1 h at 500 °C with a heating rate 10 °C min^{-1}. All of the catalytic measurements were done after 20 h conducting of the reaction. Carbon monoxide conversion value, product distribution and their concentration were determined by chromatographic analysis (GC–MS, GC with TCD or FID detector). The quantitative analysis of CO conversion (K_{CO}) and selectivity towards CO_2 (S_{CO_2}), CH_4 (S_{CH_4}), C_2H_6 ($S_{C_2H_6}$), C_3H_8 ($S_{C_3H_8}$), C_4H_{10} ($S_{C_4H_{10}}$) and liquid products (S_{LP}) were calculated in the following patterns:

$$K_{CO} = \left(\frac{X_{products}}{X_{CO_{in}}}\right) \times 100\%$$

$$S_i = \frac{X_i \times 100\%}{X_{products}}$$

Here K_{CO} is CO conversion; $X_{products}$ is the moles of all the products; $X_{CO_{in}}$ is the moles of CO on inlet before reaction (standard), S_i is the selectivity to the product; X_i is the moles of each product.

Results and discussion

The hydrogenation of carbon monoxide was performed over monometallic iron supported catalysts containing various content of Fe at various temperature of the reaction under elevated pressure (30 atm.). The catalytic activity results obtained in Fischer–Tropsch synthesis are given in Figs. 1 and 2, as well as in Tables 1 and 2. Fig. 1 presents the carbon monoxide conversion results in F–T synthesis in the temperature range 240–280 °C over 60%Fe/Al_2O_3–Cr_2O_3 (Al:Cr = 2:1). The results showed that increased of the reaction temperature result in increase of the carbon monoxide conversion value. The catalytic tests performed in F–T process at 280 °C using fixed bed reactor leads to CO conversion value above 75%. Wan et al. [3] also studied iron catalysts in Fischer–Tropsch synthesis and they also obtain very high CO conversion. They have also found that the incorporation of alumina into the precipitated iron catalyst results in a strong Fe–Al_2O_3 interaction. They have also reported that these interactions have great influence on the catalytic activity in the studied reaction. Todic et al. [20] reported, that the increase of the reaction temperature and ratio between CO and H_2 increase the selectivity to methane production and leads to decrease towards C_{5+} production. Their activity and selectivity results agree well with our results presented in this work.

In the next step, we also studied the various content of the iron on the catalytic activity of the catalysts supported on the Al_2O_3–Cr_2O_3 (Al:Cr = 2:1) binary oxide system and the results are given in Fig. 2. In the same graph, the influence of the various type of the support on the catalytic activity in F–T synthesis carried out using 40%Fe catalyst in each case was also investigated. The reactivity results clearly showed that increasing of the iron loading from 20 to 60 wt% for the investigated systems supported on Al_2O_3–Cr_2O_3 (Al:Cr = 2:1) caused the increase of the CO conversion. The maximum value of the CO conversion among of all iron containing catalysts was about 75% and this value was obtained for the catalyst containing 60 wt% of Fe. The activity results performed for 40%Fe supported catalysts showed that the most active system was 40% Fe/Al_2O_3–Cr_2O_3 (Al:Cr = 2:1) system, which exhibited the carbon monoxide conversion value equal about 67%. The catalytic activity test performed under the same conditions

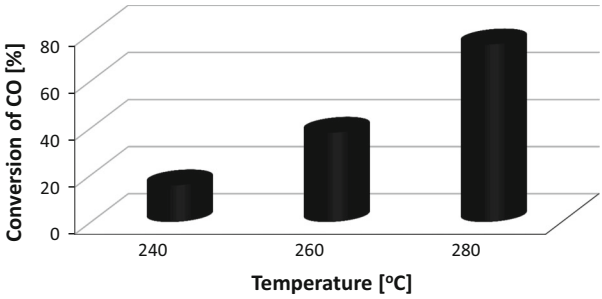

Fig. 1 The influence of the reaction temperature on the carbon monoxide conversion in F–T synthesis over 60%Fe/Al_2O_3–Cr_2O_3 (Al:Cr = 2:1) catalyst calcined in an air atmosphere at 500 °C for 4 h and reduced 1 h in a mixture of 5%H_2–95%Ar at 500 °C

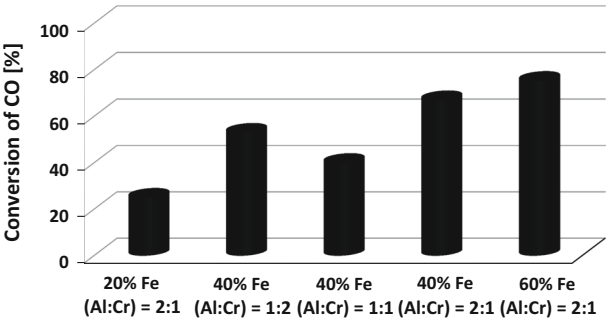

Fig. 2 The influence of the composition of the support Al_2O_3–Cr_2O_3 (Al:Cr = 2:1, 1:1, 1:2) and iron content (Fe = 20, 40, 60 wt%) in monometallic supported catalyst calcined in an air atmosphere at 500 °C for 4 h and reduced 1 h in a mixture of 5%H_2–95%Ar at 500 °C on the carbon monoxide conversion in F–T synthesis

Table 1 Distributions of the products obtained during F–T synthesis under elevated pressure (30 atm) at 240, 260 and 280 °C over monometallic iron 60%Fe/Al_2O_3–Cr_2O_3 (Al:Cr = 2:1) supported catalyst calcined in an air atmosphere at 500 °C for 4 h and then reduced 1 h in a mixture of 5%H_2–95%Ar at 500 °C

Temperature of the process °C	Products of the Fischer–Tropsch synthesis								
	CO_2 (%)	CH_4 (%)	C_2H_6 (%)	C_3H_8 (%)	C_4H_{10} (%)	C_6–C_9 (%)	C_{10}–C_{21} (%)	Liquid (%)	Gaseous (%)
240	10.2	10.6	8.2	8.0	0.0	10	53	63	37
260	33.0	14.4	9.2	5.5	1.9	6	30	36	64
280	31.9	13.0	7.8	3.2	1.1	7	36	43	57

Table 2 Distributions of the products obtained during F–T synthesis over monometallic iron catalyst containing various content of Fe supported on Al_2O_3–Cr_2O_3 (Al:Cr = 2:1, 1:1, 1:2) binary oxides under elevated pressure (30 atm) at 280 °C

Catalyst	CO_2 (%)	CH_4 (%)	C_2H_6 (%)	C_3H_8 (%)	C_4H_{10} (%)	C_6–C_9 (%)	C_{10}–C_{21} (%)	Liquid (%)	Gaseous (%)
20%Fe/Al_2O_3–Cr_2O_3 (2:1)	31.9	30	17.3	4.8	1.9	1.1	13	14	86
40%Fe/Al_2O_3–Cr_2O_3 (2:1)	27.6	13.8	9.1	4.1	1.4	11	33	44	56
40%Fe/Al_2O_3–Cr_2O_3 (1:1)	43.2	24	13.5	5.3	2.0	3	9	12	88
40%Fe/Al_2O_3–Cr_2O_3 (1:2)	40.4	21.5	13.2	5.8	2.1	2	15	17	83
60%Fe/Al_2O_3–Cr_2O_3 (2:1)	31.9	13.0	7.8	3.2	1.1	7	36	43	57

over iron catalyst containing 20 wt% of Fe (20%Fe/Al_2O_3–Cr_2O_3 (Al:Cr = 2:1)) showed that the CO conversion value was equal about 25%. Table 1 presents the distributions of the all products including also liquid hydrocarbons, obtained during CO hydrogenation process in temperature range 240–280 °C over 60%Fe/Al_2O_3–Cr_2O_3 (Al:Cr = 2:1) catalyst. The obtained activity results gave evidence that an increase in the reaction temperature leads to gaseous hydrocarbon formation, which is presented in Table 1. The highest concentration of methane was detected in the gaseous products obtained during F–T synthesis independently on the reaction temperature applied during the process. It is worth emphasizing that the higher content of the liquid products obtained in the studied process was observed in the case of the reaction performed at the lowest temperature.

This result is not applicable enough for commercial applications due to the low conversion of the CO feedstock to liquid products, especially to petrol or diesel fractions. It is worth noting that in the case of the process carried out over 60%Fe/Al_2O_3–Cr_2O_3 (Al:Cr = 2:1) catalyst at 240 °C the highest diesel fraction was obtained. On the other hand, F–T process carried out at higher temperature leads to higher gaseous product formation, which is mostly carbon dioxide and methane. The other products, which were detected by the GC system, were aliphatic hydrocarbons such as ethane, propane and butane. To sum up all of the obtained activity results presented in Table 1, we can conclude that the most applicable reaction temperature is 280 °C. On the one hand, we have obtained the highest content of gaseous products in the final product, but on the other hand, at this temperature, also the highest conversion of CO was detected. That is why we decided to use this temperature for further catalytic experiments, which were performed in the studied process.

Table 2 presents the detailed analysis of the gaseous and liquid products obtained during F–T synthesis carried out at 280 °C under 30 atm over various iron containing catalytic systems. The activity measurements given on the Table 2 showed that among of the all iron catalysts containing 40 wt% of Fe, the catalyst supported on Al_2O_3–Cr_2O_3 (2:1) system exhibited the highest liquid hydrocarbons in the final product. It is also worth mentioning that the same system showed the highest CO conversion value compared to the rest of the iron catalysts supported on other supports. This result confirmed that from the application point of view, such system is the most appropriate catalyst for diesel fraction of hydrocarbons production. This suggestion was made based on the distributions of the hydrocarbons formed in the studied reaction. The distributions of the obtained compounds gave evidence, that the smallest amount of CO_2 and the highest quantity of hydrocarbons containing 10 or more carbon atoms in a molecule are formed during F–T synthesis performed on 40%Fe/Al_2O_3–Cr_2O_3 (2:1) catalyst.

Further analysis of the obtained product in the F–T synthesis showed, that the highest desired of the unsaturated and branched hydrocarbons are formed during the process realized over iron catalyst supported on the Al_2O_3–Cr_2O_3 (2:1) binary oxide. This also suggests that this type of the support is the most suitable binary oxide systems from the application point of view for Fischer–Tropsch synthesis in order to diesel fraction production. Fig. 3 presents all of the hydrocarbons formed during the F–T process over various iron supported catalyst.

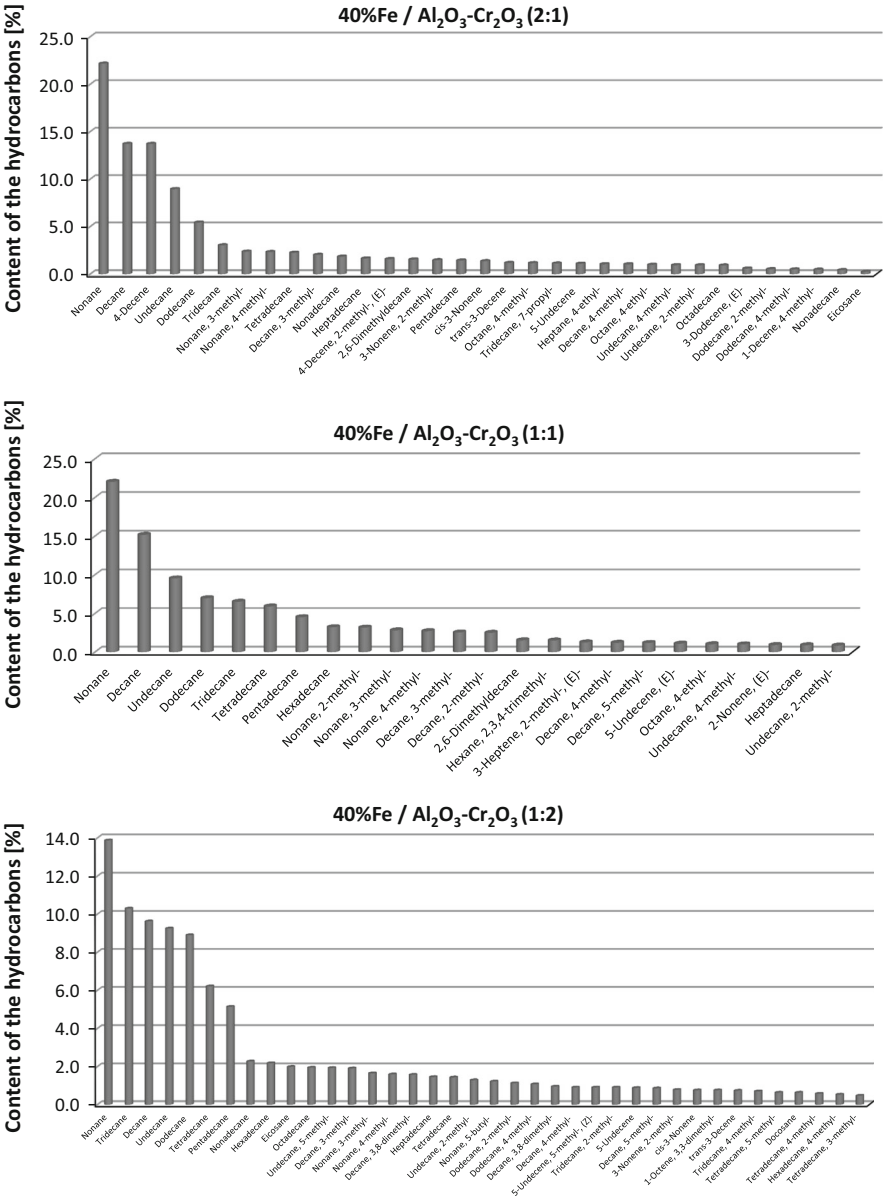

Fig. 3 Distributions of all hydrocarbons occurring in a liquid product obtained during F–T process over various monometallic iron supported catalysts

Generally, it should be noticed that the highest quantities of the branched and unsaturated linear hydrocarbons were formed over 40%Fe/Al_2O_3–Cr_2O_3 (2:1) supported catalyst (see also Table 3). It is easily observed from the presented results obtained by the GC–MS analysis of the liquid product, that the highest quantities of

Table 3 Distributions of the hydrocarbons in the liquid product formed over iron supported catalysts in Fischer–Tropsch synthesis

Type of the hydrocarbons	40%Fe/Al_2O_3–Cr_2O_3 (2:1)	40%Fe/Al_2O_3–Cr_2O_3 (1:1)	40%Fe/Al_2O_3–Cr_2O_3 (1:2)
Linear hydrocarbons (%)	70.7	74.7	75.2
Branched hydrocarbons (%)	24.4	23.3	21.6
Unsaturated hydrocarbon (%)	4.9	2.0	3.2

nonane, decane, undecane and dodecane hydrocarbons were formed in all cases. It is also worth noticing that the heaviest hydrocarbon formed during the F–T process was eicosane in all cases. This result confirmed that also some parts of the obtained product were paraffin waxes in addition to gaseous and liquid hydrocarbons. We also studied the distributions of the hydrocarbons in the liquid products obtained during the Fischer–Tropsch synthesis by FTIR technique in this work (Fig. 3).

The analysis of the liquid product obtained during the Fischer–Tropsch synthesis showed that alkanes, aliphatic and branched hydrocarbons are formed in F–T process independently on the catalyst applied during the reaction. In the next part of the analysis of the final liquid product obtained during the F–T synthesis we carried out FTIR measurements for these products and the results are given in Fig. 4. The FTIR spectra obtained for liquid products produced during F–T synthesis realized on iron containing catalyst supported on various binary oxides Al_2O_3–Cr_2O_3 confirmed the occurrence of the same types of the hydrocarbons in the final product, which were detected by the GC–MS technique. The FTIR analysis of the liquid product confirmed the presence of the functional groups which allow confirming the occurrence of alkanes, branched and linear aliphatic hydrocarbons in the F–T product formed during the synthesis [21]. In the FTIR spectra recorded for all iron supported catalysts independently on the composition of the support, the specific bands which attributable to surface species such as –OH stretching, –C–H stretching in alkanes, C–H in alkenes, C=C in alkenes, $–CH_2$, –CH, $–CH_3$, R–CH=CH–R, $(CH_2)n > 4$ were detected. The occurrence of these bands on the FTIR spectra confirmed the GC–MS results.

To understand the activity row of the monometallic iron supported catalysts in Fischer–Tropsch synthesis, specific surface area (SSA) measurements were done. The results of the SSA obtained for binary oxide supports and monometallic iron supported catalysts were given in Fig. 5 and Table 4. Fig. 5 presents the pore size distributions for all catalytic materials.

The results of pore size distributions showed that the Al_2O_3–Cr_2O_3 (2:1) system showed the average pore radius of about 2.6 nm. On the other hand, the rest of the binary oxides containing lower content of alumina exhibited lower surface area and lower average pore size equal 1.9 and 2.1 nm for Al_2O_3–Cr_2O_3 (1:2) and Al_2O_3–Cr_2O_3 (1:1) systems.

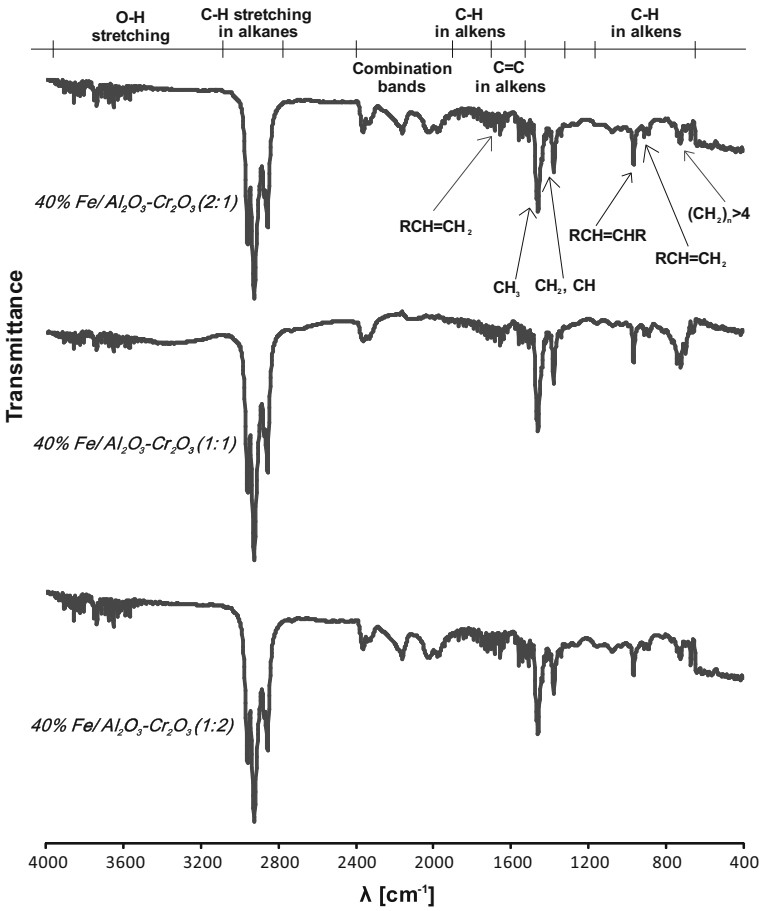

Fig. 4 FTIR spectra of liquid products obtained in F–T process over iron catalysts supported on various binary oxides calcined at 500 °C in an air atmosphere for 4 h

In the case of the monometallic supported catalysts, the same tendency was observed. The highest specific surface area exhibited the catalytic system supported on the binary oxide Al_2O_3–Cr_2O_3 (2:1). The same monometallic supported catalysts showed also the lowest average pore radius among of all monometallic catalysts (2.6 nm). While the rest of the iron catalyst had the average pore radius equal 5.5 nm. It is also worth mentioning that the catalyst which was characterized by the highest specific surface area also showed the highest CO conversion in F–T synthesis among all of the iron catalyst containing the same loading 40 wt% of Fe.

In the next step of our measurements, we decided to study the reducibility of the supports and iron containing systems. First of all, we studied the reducibility of the supports systems. The TPR–H_2 measurements performed for all supports showed that all binary oxides are reduced in one single step (see Fig. 6). This single

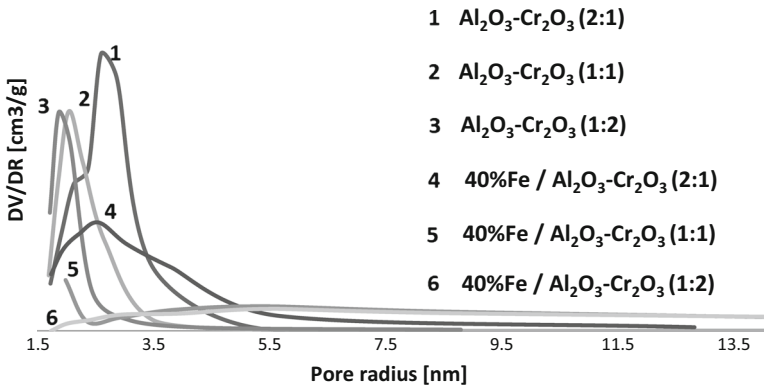

Fig. 5 Pore radius distributions for supports (Al_2O_3–Cr_2O_3 (1:1), Al_2O_3–Cr_2O_3 (1:2), Al_2O_3–Cr_2O_3 (2:1)) calcined at 400 °C in air atmosphere for 4 h and monometallic iron supported catalysts calcined at 500 °C in air atmosphere for 4 h

Table 4 Specific surface area and average pore radius for supports calcined in air atmosphere for 4 h at 400 °C and monometallic supported iron catalysts calcined in air atmosphere for 4 h at 500 °C

Catalyst	Specific surface area ($m^2\ g^{-1}$)	Average pore radius (nm)
Al_2O_3–Cr_2O_3 (1:2)	91	1.9
Al_2O_3–Cr_2O_3 (1:1)	131	2.1
Al_2O_3–Cr_2O_3 (2:1)	251	2.6
40%Fe/Al_2O_3–Cr_2O_3 (1:2)	44	5.5
40%Fe/Al_2O_3–Cr_2O_3 (1:1)	52	5.5
40%Fe/Al_2O_3–Cr_2O_3 (2:1)	118	2.6

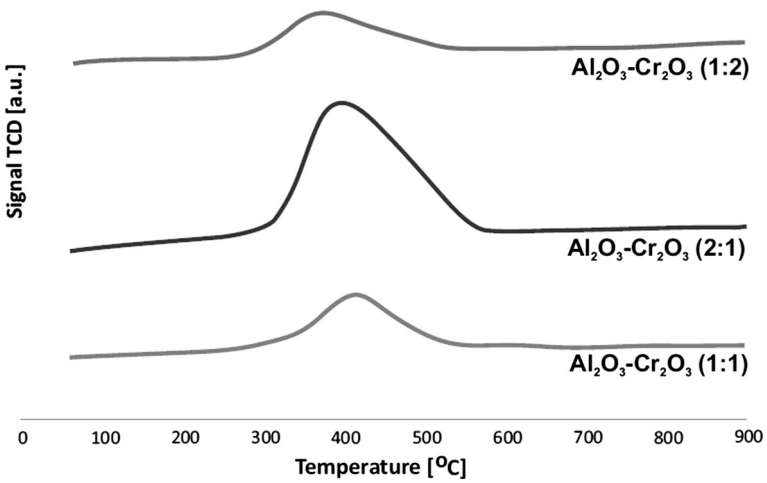

Fig. 6 TPR–H_2 profiles recorded for binary oxide systems containing different content of alumina and chromium which have been also calcined in an air atmosphere at 400 °C for 4 h

reduction stage was situated in the temperature range 300–580 °C, which is connected with the reduction of Cr(VI) oxidized phase formed from the previously re-oxidized phase of Cr_2O_3 [22–26]. The obtained results also clearly indicate that the highest hydrogen consumption peak was observed for Al_2O_3–Cr_2O_3 (2:1) system. In the next step, we would like to elucidate the interaction between the active phase and the support and we investigated the reduction behavior of iron catalysts 40%Fe/Al_2O_3–Cr_2O_3 (2:1) supported on previously prepared binary oxide. To understand the reduction behavior of the monometallic supported catalyst better, we carried out also the reduction study for pure hematite. The results of the reducibility obtained for hematite and iron supported catalysts are presented in Fig. 7.

The reduction profile recorded for hematite showed three reduction stages connected with the reduction of Fe_2O_3 to metallic iron through the intermediates such as Fe_3O_4 and FeO. The first reduction stage situated in the temperature range 250–350 °C is connected with the reduction of Fe_2O_3 to Fe_3O_4 (magnetite) [14]. The second reduction peak is assigned to the reduction of magnetite phase to wustite FeO and the last hydrogen consumption peak with the maximum at about 700 °C is attributed to the reduction of FeO to metallic iron. Many researchers [27–29] also studied iron catalysts by temperature programmed reduction technique and they also observed three reduction stages on the TPR–H_2 profile. They reported about the same reduction stages during the reduction process of hematite. However, in the case of the monometallic iron supported catalyst, analogous reduction stages were also observed on the TPR–H_2 profile recorded for monometallic catalyst 40%Fe/Al_2O_3–Cr_2O_3 (2:1). The TPR–H_2 profile recorded for monometallic catalyst showed three reduction stages with the maximum of the hydrogen consumption peak at 250, 350 and 550 °C. It is also worth mentioning that well resolved reduction peaks are the result of a low heating rate (1 °C min^{-1}) applying during the reduction process in the case of the monometallic catalyst.

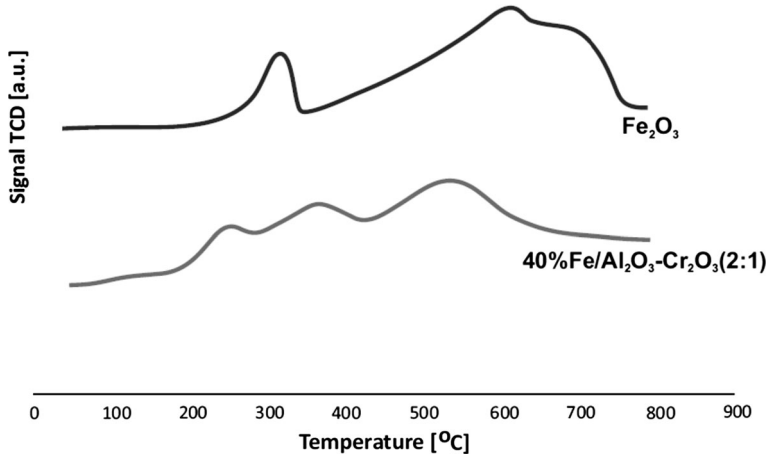

Fig. 7 TPR–H_2 profiles recorded for hematite and iron catalyst supported on binary oxide system (Al_2O_3–Cr_2O_3 (2:1)) calcined in an air atmosphere at 500 °C for 4 h

The influence of the acidity on the catalytic activity in Fischer–Tropsch synthesis was also studied in this work. The acidity measurements were also carried out for supports and monometallic iron supported catalysts and the results are given in Table 5. The results of the acidity measurements clearly showed that the highest acidity exhibited binary oxide Al_2O_3–Cr_2O_3 (2:1) which owned the highest specific surface area and contain the highest content of alumina. Additionally, all of the investigated catalytic systems exhibited three various acidic centres on their surface. It is also worth mentioning that also among of the iron supported catalysts the most acidic system proved to be 40%Fe/Al_2O_3–Cr_2O_3 (2:1) catalyst. These results indicate that this system exhibited the highest electron acceptor properties. In addition, the acidity results correlate well with the activity measurements. The most active catalyst was system which was characterized by the highest total acidity compared to the rest of the monometallic iron supported catalysts. In addition, the catalyst which exhibited the highest acidity among all catalytic systems also showed higher isomerization activity (see Table 3 and Fig. 3) [21]. The analogical results were obtained by Abramova et al. [30]. They reported that zeolite catalysts which owned higher quantity of the acidic centers with medium strength showed also higher isomerization activity in Fischer–Tropsch synthesis. Prieto et al. [31] claimed that the overall reaction rate of the F–T synthesis carried out on cobalt catalysts reaches a maximum for oxide supports characterized by an intermediate acid–base character. Such activity behaviour authors related with the nature of the support. This tendency is related to the correlation of the number of surface-exposed cobalt sites and their intrinsic activity.

In order to explain the reactivity results in Fischer–Tropsch synthesis SEM–EDS measurements for iron containing catalysts were carried out and the results are given in Fig. 8. The SEM–EDS measurements showed that in all cases all of the catalyst components such us Fe, Al, Cr and O were visible on the SEM images. The main

Table 5 The amount of NH_3 adsorbed on binary oxide supports calcined in air atmosphere for 4 h at 400 °C and monometallic iron supported catalysts calcined in air atmosphere for 4 h at 500 °C from the TPD–NH_3 data

Catalysts/supports	Weak centers (mmol g^{-1})	Medium centers (mmol g^{-1})	Strong centers (mmo g^{-1})	The total amount of desorbed NH_3 (mmo g^{-1})
Al_2O_3–Cr_2O_3 (2:1)	0.49	0.51	0.69	1.69
Al_2O_3–Cr_2O_3 (1:1)	0.21	0.27	0.34	0.82
Al_2O_3–Cr_2O_3 (1:2)	0.07	0.01	0.01	0.09
40%Fe/Al_2O_3–Cr_2O_3 (2:1)	0.16	0.16	0.21	0.53
40%Fe/Al_2O_3–Cr_2O_3 (1:1)	0.04	0.06	0.08	0.18
40%Fe/Al_2O_3–Cr_2O_3 (1:2)	0.04	0.03	0.06	0.13

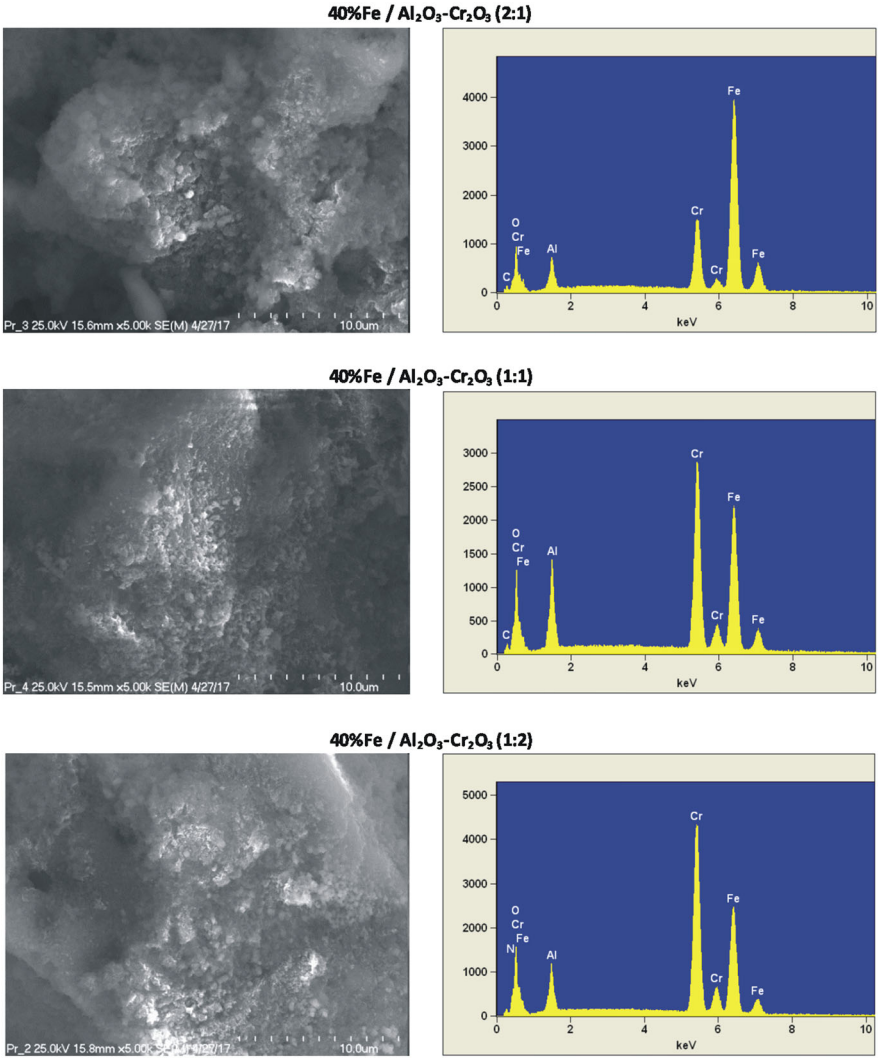

Fig. 8 SEM images and EDS spectra collected for the 40%Fe/Al_2O_3–Cr_2O_3 (2:1), 40%Fe/Al_2O_3–Cr_2O_3 (1:1), 40%Fe/Al_2O_3–Cr_2O_3 (1:2)

information from the performed experiments is the fact that for the 40%Fe/Al_2O_3–Cr_2O_3 (2:1) catalyst which exhibited the highest activity in the studied reaction, the highest content of the iron species were detected on the catalyst surface.

In order to determine the phase composition studies of the iron supported catalysts XRD measurements were performed and the results are presented in Fig. 9. The results obtained for the catalysts reduced for 2 h at 500 °C in a mixture of 5%H_2–95%Ar atmosphere showed that on the diffraction curves recorded for them the presence of Fe_3O_4, $FeCr_2O_4$ and α-Cr_2O_3 phases were detected. It is also worth noticing that on the XRD curve recorded for the catalyst which showed the

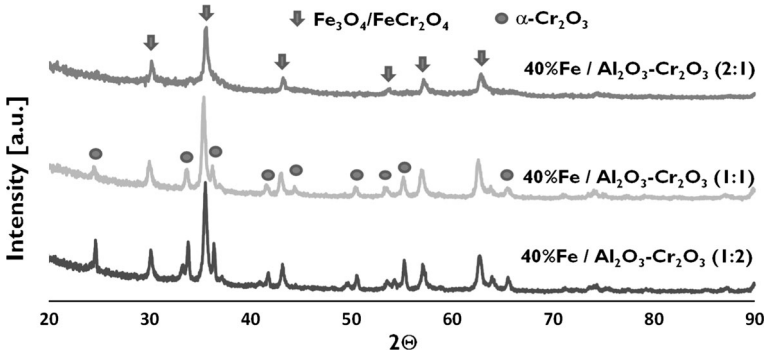

Fig. 9 XRD patterns recorded for iron catalysts supported on various binary oxides previously reduced in a mixture of 5%H_2–95Ar at 500 °C for 1 h

highest activity only diffraction peaks attributed to Fe_3O_4 and $FeCr_2O_4$ phases were observed. The presence of such phases agrees well with the SEM–EDS measurements, which were obtained for the iron supported catalysts. These results can also explain the reactivity results of the iron supported catalysts tested in Fischer–Tropsch synthesis.

To further confirm the special interaction between chromium oxide and aluminum oxide and also the formation of the magnetite or iron chromite phases on the iron catalyst surface, ToF–SIMS measurements for binary oxides and iron supported catalyst were performed. The results of the TOF–SIMS measurements are presented in Table 6. The results recorded for binary oxides showed the presence of $CrAlO^+$ surface ions, which confirm the presence of the specific interactions between

Table 6 TOF–SIMS results obtained for binary oxides systems reduced in an atmosphere of 5%H_2–95%Ar at 500 °C for 1 h

Al_2O_3–Cr_2O_3 (1:1)		Al_2O_3–Cr_2O_3 (1:2)		Al_2O_3–Cr_2O_3 (2:1)		40%Fe/Al_2O_3–Cr_2O_3 (2:1)	
Ion (mass number)	Number of counts	Ion (mass number)	Number of counts	Ion (mass number)	Number of counts	Ion (mass number)	Number of counts
Al^+ (27)	966313	Al^+ (27)	1203442	Al^+ (27)	1362940	Al^+ (27)	947687
AlO^+ (43)	3952	AlO^+ (43)	4711	AlO^+ (43)	7058	AlO^+ (43)	3862
Cr^+ (52)	496895	Cr^+ (52)	796694	Cr^+ (52)	652143	Cr^+ (52)	309445
CrO^+ (68)	52783	CrO^+ (68)	95806	CrO^+ (68)	97863	Fe^+ (56)	223633
$CrAlO^+$ (95)	10090	$CrAlO^+$ (95)	15350	$CrAlO^+$ (95)	13989	CrO^+ (68)	37053
–	–	–	–	–	–	FeO^+ (72)	11022
–	–	–	–	–	–	$CrAlO^+$ (95)	7325
–	–	–	–	–	–	$AlFeO^+$ (99)	10689
–	–	–	–	–	–	$CrFeO^+$ (124)	6775

chromium and aluminum oxides. Additionally, the presence of the AlO^+ and CrO^+ ions on the TOF–SIMS spectra of the catalyst indicates the occurrence of alumina and chromium oxide in binary systems. The morphology and the surface composition of the monometallic supported iron catalyst were also studied in this work. The collected TOF–SIMS spectra from the surface of the investigated catalyst system gave evidence, that on the surface of this catalyst after reduction the occurrence of the same oxide species which were detected for the binary oxide system Al_2O_3–Cr_2O_3 (2:1) were confirmed. In addition, in the case of 40%Fe/Al_2O_3–Cr_2O_3 (2:1) system the presence of $AlFeO^+$ and $CrFeO^+$ ions were detected. The presence of these ions indicates the formation of specific interaction between iron oxide and alumina or iron and chromium oxides. These measurements confirmed the XRD results obtained for iron supported catalyst and agree well with our previous findings.

Conclusions

The monometallic iron supported catalysts were prepared by impregnation method and tested in F–T process. The catalytic activity tests showed that the distributions of the hydrocarbons in the final product depend strongly on the type of supports and its acidity and reducibility properties. The analysis of the reactivity results gave evidence that the most suitable monometallic iron system for F–T synthesis was 40%Fe/Al_2O_3–Cr_2O_3 (2:1) catalyst. This result is explained by the presence of the highest concentration of Fe species on its surface. Fe species on the surface are the active centers of the investigated process. In addition, this system exhibited the highest specific surface area, which also means that it had the highest dispersion of the iron species on the catalyst surface. It was also confirmed that the 40%Fe/Al_2O_3–Cr_2O_3 (2:1) catalyst showed the highest quantity of the magnetite and iron chromite phases on its surface after reduction process performed in a mixture of 5%H_2–95%Ar performed at 500 °C for 1 h. The presence of these compounds was confirmed by ToF–SIMS analysis performed for the reduced monometallic supported catalyst system. The GC–MS and FTIR analysis showed that the liquid product obtained in F–T synthesis contained only alkanes, alkenes and branched hydrocarbons. The increase of the reaction temperature leads to gaseous compounds formation in F–T synthesis, especially CO_2, which is formed via the WGS reaction.

Acknowledgements This work was partially funded from NCBiR (Grant No. BIOSTRATEG2/297310/13/NCBiR/2016).

Compliance with ethical standards

Conflict of interest The authors declare that they have no conflict of interest.

References

1. Khodakov AY, Lynch J, Bazin D, Rebours B, Zanier N, Moisson B, Chaumette P (1997) J Catal 168:16–25
2. Schulz H (1999) Appl Catal A 186:3–12
3. Wan H-J, Wu B-S, Zhang C-H, Xiang H-W, Li Y-W, Xu B-F, Yi F (2007) Catal Commun 8:1538–1545
4. Riedel T, Schulz H, Schaub G, Jun K-W, Hwang J-S, Lee K-W (2003) Top Catal 26:41–54
5. Dry ME (1990) Catal Lett 7:241–251
6. Davis BH (2009) Catal Today 141:25–33
7. Mierczynski P, Maniecki T, Kaluzna-Czaplinska J, Szynkowska M, Maniukiewicz W, Lason-Rydel M, Jozwiak WK (2013) Cent Eur J Chem 11:304–312
8. Khodakov AY, Chu W, Fongarland P (2007) Chem Rev 107:1692–1744
9. Chernavskii PA, Pankina GV, Lermontov AS, Lunin VV (2003) Kinet Catal 44:657–661
10. Savost'yanov AP, Yakovenko RE, Narochnyi GB, Bakun VG, Sulima SI, Yakuba ES, Mitchenko SA (2017) Kinet Catal 58:81–91
11. Chalupka KA, Maniukiewicz W, Mierczynski P, Maniecki T, Rynkowski J, Dzwigaj S (2015) Catal Today 257:117–121
12. Chernavskii PA, Kazak VO, Pankina GV, Lunin VV (2016) Kinet Catal 57:333–338
13. Ding F, Zhang A, Liu M, Zuo Y, Li K, Guo X, Song C (2014) Ind Eng Chem Res 53:17563–17569
14. Suo H, Wang S, Zhang C, Xu J, Wu B, Yang Y, Xiang H, Li Y-W (2012) J Catal 286:111–123
15. Mierczynski P, Chalupka KA, Maniukiewicz W, Kubicki J, Szynkowska MI, Maniecki TP (2015) Appl Catal B 164:176–183
16. Mierczynski P (2016) Catal Lett 146:1825–1837
17. Maniecki T, Bawolak-Olczak K, Mierczynski P, Maniukiewicz W, Jozwiak WK (2009) Chem Eng J 154:142–148
18. Pérez-Alonso FJ, Granados ML, Ojeda M, Herranz T, Rojas S, Terreros P, Fierro JLG, Gracia M, Gancedo JR (2006) J. Phys Chem B 110:23870–23880
19. Arsalanfar M, Mirzaei AA, Bozorgzadeh HR (2012) J Nat Gas Sci Eng 6:1–13
20. Todic B, Nowicki L, Nikacevic N, Bukur DB (2016) Catal Today 261:28–39
21. Di Sanzo FP (1981) Anal Chem 53:1911–1914
22. Mierczynski P, Kaczorowski P, Maniecki T, Bawolak-Olczak K, Maniukiewicz W (2013) React Kinet Mech Cat 109:13–27
23. Mierczynski P, Maniecki T, Maniukiewicz W, Jozwiak W (2011) React Kinet Mech Cat 104:139–148
24. Maniecki T, Mierczynski P, Maniukiewicz W, Gebauer D, Jozwiak W (2009) Kinet Catal 50:228–234
25. Maniecki T, Mierczynski P, Maniukiewicz W, Bawolak K, Gebauer D, Jozwiak W (2009) Catal Lett 130:481–488
26. Maniecki TP, Mierczyński P, Maniukiewicz W, Jóźwiak WK (2011) Kinet Catal 52:835–842
27. Jozwiak W, Maniecki T, Mierczynski P, Bawolak K, Maniukiewicz W (2009) Pol J Chem 83:2153–2162
28. Jozwiak WK, Kaczmarek E, Maniecki TP, Ignaczak W, Maniukiewicz W (2007) Appl Catal A 326:17–27
29. Zieliński J, Zglinicka I, Znak L, Kaszkur Z (2010) Appl Catal A 381:191–196
30. Abramova AV, Panin AA, Kliger GA, Kulikova EA, Slivinsky EV (2005) Production of synthetic fuels from alternative petroleum raw material by method of Fischer–Tropsch on zeolite catalysts. Elsevier, Amsterdam, pp 1709–1716
31. Prieto G, De Mello MIS, Concepción P, Murciano R, Pergher SBC, MartÍnez AN (2015) ACS Catal 5:3323–3335